Journal of Nuclear Materials 385 (2009) 278–283

Contents lists available at ScienceDirect

Journal of Nuclear Materials

journal homepage: www.elsevier.com/locate/jnucmat

The hardening of iron–chromium alloys under thermal ageing: An atomistic study

G. Bonny [a,b,*], D. Terentyev [a], L. Malerba [a]

[a] SCK-CEN, Nuclear Materials Science Institute, Boeretang 200, B-2400, Mol, Belgium
[b] Ghent University, Center for Molecular Modeling, Proeftuinstraat 86, B-9000 Gent, Belgium

ARTICLE INFO

PACS:
64.75.Nx
62.20.−x
64.60.Q−

ABSTRACT

In this work an atomistic multi-scale modelling approach is applied to study: (i) the kinetics of phase separation during thermal ageing of binary Fe–Cr alloys and (ii) the interaction of dislocations with Cr-rich precipitates. The studies were performed varying the Cr content in the range of 12–18 at.% Cr and at temperatures from 600 to 900 K, which is within the miscibility gap where phase separation occurs. Thermal ageing was simulated using atomistic kinetic Monte Carlo techniques while the interaction of a dislocation with Cr-rich precipitates was studied by molecular dynamics. In both cases the description of atomic interactions was provided by the same semi-empirical interatomic potential, partially fitted to available *ab initio* data. Both studies are combined to analyse the hardening of Fe–Cr alloys during thermal ageing.

1. Introduction

Fe–Cr alloys are the base for ferritic and ferritic/martensitic (F&FM) steels, which have a wide range of applications as structural materials in aggressive high temperature environments, such as gas turbines in conventional power plants, or key components in future nuclear reactors. Binary Fe–Cr alloys and F&FM steels undergo α–α' phase separation if the Cr content, x_{Cr}, exceeds ~9 at.% Cr (henceforth %), in the region of temperatures potentially important for technological applications (>700 K) [1–10]. The formation of finely-dispersed, nanometric-size, coherent Cr-rich precipitates in the bulk and at dislocations is long since known to be the cause of hardening and embrittlement of F&FM steels with $x_{Cr} > 14\%$ after thermal ageing (so-called "475 °C embrittlement" [1–5]), as well as, at even lower temperature and Cr content, under irradiation, which is found to accelerate the phase separation process [7,9,10], or possibly induce it [11–13]. Therefore, a quantitative understanding of the kinetics of α–α' decomposition and its impact on mechanical property changes in Fe–Cr alloys is an important issue to be addressed.

Experiments involving thermal ageing are time consuming (up to years), especially at relatively low temperature (⩽800 K) and at x_{Cr} near the solubility limit. For a rigorous and reliable study, different experimental techniques should be combined, which is expensive. This is probably why very few experimental works providing detailed information about the different stages of α–α' unmixing are available in the literature, particularly in Fe–Cr alloys in the range of compositions of technological application in power plants, i.e. <20% Cr (most work on model alloys was devoted to the study of spinodal decomposition, well above such concentrations, see [14] for a review). Only a couple of small angle neutron scattering (SANS) studies were found on thermally aged Fe–20 Cr [6,8], that reach a good level of detail, but are not backed by any other relevant technique, such as tomographic atom probe (TAP). For the rest, a few SANS studies exist on steels with less than 20% Cr, but again not supported by other techniques and largely dealing with irradiation effects, without tracing the microstructure evolution (only the final situation is reported) [9,10]. In experiments involving irradiation it is in addition difficult to distinguish between the impact on mechanical properties of Cr-rich precipitates and other irradiation-induced defects or other types of precipitates. In thermally aged model alloys, only a couple of early attempts have been done to correlate the kinetics of α' precipitation with the corresponding hardening, but without actually using any real microstructural information [4,5].

While efforts are being made in the international scientific arena to fill this gap of missing experimental data, computer simulation studies can contribute to the understanding of microstructure evolution and its relation with mechanical property changes. The degradation of materials due to α–α' decomposition is a multi-scale process, in which atomic-scale features (precipitates) or phenomena (diffusion) directly impact macroscopic properties (hardening, embrittlement). The timescale of precipitation under ageing conditions is of the order of thousands or tens of thousands of hours [1–5,7–10], whereas the response of the component to a load exceeding the limits of resistance by plastic deformation is provided in fractions of a second. Nowadays, it is widely accepted that a multi-scale modelling approach may provide a practical framework to tackle problems of this kind. More to the point, it has been recently shown that existing hardening models and

* Corresponding author. Address: SCK-CEN, Nuclear Materials Science Institute, Boeretang 200, B-2400, Mol, Belgium. Tel.: +32 14 333198; fax: +32 14 321216.
E-mail address: gbonny@sckcen.be (G. Bonny).

0022-3115/$ - see front matter © 2008 Elsevier B.V. All rights reserved.
doi:10.1016/j.jnucmat.2008.12.002

correlations (based on elasticity theory) are not suitable to properly treat the hardening effect due to small Cr-rich precipitates, therefore requiring the use of atomic-level techniques [15]. In the present work such an approach is used to attempt the study of α–α' phase separation during thermal ageing in Fe–Cr and its impact on mechanical properties changes.

Atomistic kinetic Monte Carlo (AKMC) methods are used to simulate bulk thermal ageing in Fe–Cr crystals, where the cohesive model is provided by a density functional theory (DFT)-based interatomic potential. The atomic configurations after heat treatment then serve as input for molecular dynamics (MD) simulations, where the same interatomic potential is used to study the effect of phase separation on the dislocation motion at the atomic-level.

Eventually, the information thereby obtained could be transferred to mesoscopic models, such as dislocation dynamics (DD), thereby bridging from the atomic/micro-scale to the meso/macro-scale comparable with experiments.

2. Background and methodology

2.1. Appropriate cohesive model

The thermodynamic properties of Fe–Cr alloys are partially driven by a complex magnetic interaction [16], which is challenging to model at scales beyond those accessible to DFT calculations. Due to magnetism, a change of the sign in the heat of mixing occurs, which is negative below a critical concentration and positive above it. As a consequence, Cr atoms have a tendency to order or to form clusters, depending on the alloy composition. Different DFT approximations suggest the critical concentration to be between 4% and 10% of Cr [17–19]. For our study, it is essential that the above mentioned properties are well reproduced by the cohesive model implemented in the AKMC and MD codes.

In the literature three different DFT-based cohesive models exist that reproduce fairly well the Fe–Cr thermodynamic properties, even though none of them includes magnetism explicitly [19]. These are: a concentration-dependent model (CDM) by Caro et al. [20], a two-band model (2BM) by Olsson et al. [21] and a cluster expansion model (CEM) by Lavrentiev et al. [22]. The two former models are *ad hoc* extensions of the standard embedded atom method (EAM) [23], where an additional term that depends on local solute concentration is introduced. The CEM provides an energy model for a rigid lattice, therefore making it unsuitable for MD simulations where the displacement of the atoms from their equilibrium lattice sites is of concern. Among the CDM and 2BM, the latter is selected since it is the only model predicting a composition of α' precipitates in agreement with experimental observations [19,24], i.e. containing a few percents of Fe [1–3,9,10,25–27], rather than being pure Cr, as predicted by the other two models [20,22].

2.2. Simulation of thermal ageing

The thermal ageing was modelled using a rigid lattice AKMC technique [28]. The evolution of the system was driven by single vacancy diffusion, performing migration jumps at a rate,

$$\Gamma = n_0 \exp(-E_m/k_B T). \quad (1)$$

Here n_0 is an attempt frequency (taken as $6 \times 10^{12}\ s^{-1}$ independently of Cr content and temperature), E_m is the local atomic environment (LAE)-dependent migration energy, k_B is the Boltzmann constant and T is the absolute temperature. The dependence of E_m on LAE was introduced as $E_m = E_0 + \Delta E_{f-i}/2$, where ΔE_{f-i} is the total energy change due to the vacancy jump and E_0 is the excess migration energy [28,29]. E_0 is taken as the migration barrier for an Fe (Cr) atom exchanging position with the vacancy, calculated by DFT (in the limit of dilute solution [30]): 0.65 and 0.55 eV for the Fe and Cr species, respectively. In a body-centered-cubic (bcc) lattice, eight possible sites (first nearest neighbours) are accessible to the vacancy exchange jump (exchanges with farther neighbours require much higher migration energy). Each jump corresponds to one AKMC step. The related elapsed time at each jump, Δt_{MC}, is calculated using the averaged residence time algorithm, as the inverse of the sum of the eight possible jump frequencies [31].

The Cr-concentration x_{Cr} and temperature T were chosen to be within the miscibility gap where α–α' phase separation is expected to occur, and also to be relevant for technological nuclear applications: 12–18% Cr and 600–900 K. Initially, Cr atoms were randomly distributed in a bcc Fe matrix with size $40 \times 40 \times 40$ cubic cells, containing 128 000 atoms in total. The thermal annealing was simulated up to $1–2 \times 10^{10}$ AKMC steps (depending on temperature), until the coarsening regime is established (note that in the closest experiments to our simulations only the coarsening stage is observed [6,8]). This corresponded to a Monte Carlo time, t_{MC}, ~130, 14, 4 and 1 s for 600, 700, 800 and 900 K, respectively, whose correlation with real time is a debated matter [32]. Each simulation was performed twice, using different seeds for the initial Cr distribution.

2.3. Microstructure analysis

The atomic configurations obtained from the AKMC simulations were post-processed to characterize the precipitation process, by applying the methodology developed by the authors in [24] to identify non-pure coherent precipitates in concentrated solid solutions. The latter is based on the assignment of an on-site concentration (within fifth nearest neighbour shell) to each atom and the selection of those with a concentration higher than a given threshold (here 94% Cr). The bases for the selection of the threshold are discussed in [24]. This allows precipitates to be identified and therefore the size and density distribution at any AKMC step to be calculated.

2.4. Simulation of dislocation-precipitate interaction

The hardening related to α' precipitation has been explicitly associated with obstruction of the edge dislocations motion mainly [2], thus this type of dislocation-precipitate interaction has been studied here using MD simulations. A $1/2[1\,1\,1]\,(1\bar{1}0)$ edge dislocation (henceforth dislocation) was constructed following the procedure proposed in [33] and set into motion by applying $[1\,1\,1]\,(1\bar{1}0)$ shear strain γ at constant rate of $10^{-5}\ ps^{-1}$. The corresponding stress–strain relationships were obtained by estimating the stress acting on the fixed parts of the MD crystallite subjected to displacement [15,33]. Nearly-spherical Cr-precipitates, with size and density as found in the AKMC simulations, were placed in Fe–9 Cr matrices (almost temperature-independent α-phase composition after phase separation in the studied range of temperatures) so that the dislocation intersected the precipitate at its equator. Accounting for the precipitate size distributions obtained from the AKMC simulations, reactions with precipitates of size that, varied from 0.5 to 3.5 nm in diameter were considered. The reactions were modelled in crystals with dimensions $28.9 \times 19.8 \times 24.8\ nm^3$ and $41.4 \times 19.8 \times 24.8\ nm^3$, along $[11\bar{2}]$, $[1\bar{1}0]$ and $[1\,1\,1]$ directions, respectively. The centre-to-centre obstacle spacing, L_D, was 28.9 and 41.4 nm. The simulation temperature was varied from 300 to 900 K. The MD integration time step was taken to be 5 fs for simulations at 300 K and 1 fs at higher temperatures (i.e. 600 and 900 K). More details on similar simulations at lower temperature are given in [34].

2.5. Analytical treatment of the yield stress

The motion of the dislocation in concentrated random Fe–Cr alloys was found to occur via propagation of individual segments (with length around 10–30b), separated by some relatively strong obstacles (presumably small Cr clusters) [34] at which the dislocation line was pinned. In this situation, the stress–strain curve presents irregular peaks, due to the randomness of the dispersed Cr. The density and strength of the pinning points along the dislocation line varies while the dislocation glides through them. Thus, the determination of the friction flow stress in the alloy becomes ambiguous and simple averaging may not be suitable. An approach proposed in [35] is therefore applied, wherein the flow stress is obtained as

$$\tau_{\text{rand}} = \frac{k_B T}{V} \ln \left\langle \exp\left(\frac{V\tau}{k_B T}\right) \right\rangle \tag{2}$$

where τ is the stress coming from MD simulations, T is the simulation temperature, V is the activation volume (taken as b^3) and k_B is the Boltzmann constant. The averaging is performed over the simulation time (long enough for the dislocation to cover a distance of 300b).

When simulating precipitate-dislocation interaction, on the other hand, the critical stress needed to unpin the dislocation can be obtained unambiguously by looking at the stress before and after the dislocation is released. Each reaction was simulated five times, varying the position of the precipitate in the matrix, to allow for the effect of the local Cr distribution, accounted for via the standard deviation. The average critical stress, τ_C, needed to shear the precipitates was subsequently used to calculate the strength, α, of the precipitates vs. diameter, d_p, as

$$\tau_C = \alpha \frac{\mu b}{L'} \tag{3}$$

here μ is the shear modulus (70 GPa as in pure Fe [15]) and L' is the free dislocation passage distance ($L' = L_D - d_p$ i.e. edge-to-edge precipitate spacing). With the obtained α, the flow stress in a matrix containing a random distribution of precipitates (assuming that they are deformable obstacles, as suggested by static calculations [34]) with a given density, N_p, and mean size, $\bar{d}_p$, can be estimated as [36]

$$\tau_P = \alpha^{3/2} \frac{\mu b}{(N_p^{-1/3} - \bar{d}_p)} \tag{4}$$

Finally, to estimate the change in the flow stress, $\Delta\tau$, of the random alloy with composition x_{Cr} and the same alloy after phase separation, the matrix depletion needs to be accounted for, so

$$\Delta\tau = \tau_p^{\text{Fe-9\%Cr}} - \Delta\tau_{\text{rand}} \tag{5}$$

where the first term is the flow stress in the phase separated alloy (i.e. 9% Cr background with the precipitate) and the second term is the difference in the flow stress between the given x_{Cr} and the 9% Cr random alloy. Note that here the two hardening effects related to the solid solution and Cr-precipitates were assumed to be linearly additive. The problem of the additivity of the solid solution and precipitate hardening is addressed in [15,37].

3. Results

3.1. Thermal ageing

Applying the analysis described in Section 2.3, the precipitates were identified during thermal annealing and their density, N_p, and average diameter, $\bar{d}_p$, are presented in Figs. 1 and 2 as functions of t_{MC}, for the two extreme Ts and all x_{Cr} here studied. In Fig. 3, x_{Cr} in the matrix is plotted as a function of t_{MC}. The combined inspection of these figures enables a clear identification of the three precipitation regimes, namely: nucleation, growth and coarsening.

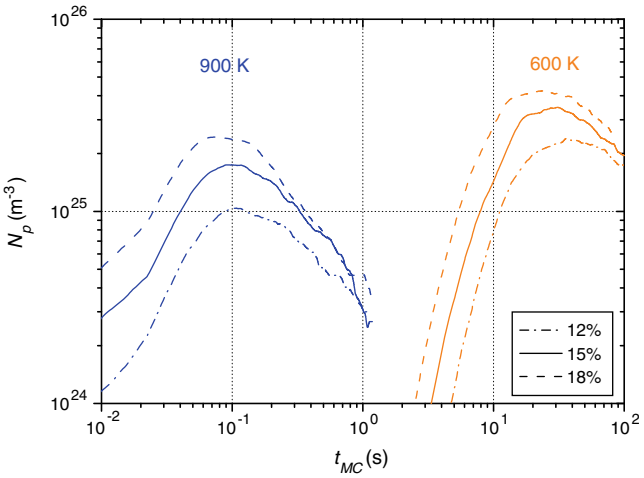

Fig. 1. The precipitate density as a function of Monte Carlo simulation time.

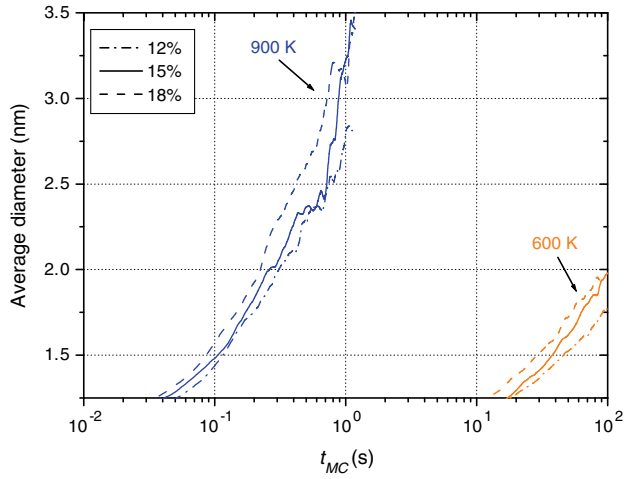

Fig. 2. The average diameter of the precipitates as a function of Monte Carlo simulation time.

A dominant nucleation regime is identified by the initial steep increase of N_p and slow growth of $\bar{d}_p$. The presence of the plateau around the peak density N_p^{max} and the simultaneous fast growth of $\bar{d}_p$ and fast depletion of Cr from the matrix is to be attributed to the onset of a growth stage. Finally, the decrease of N_p and simultaneous increase of $\bar{d}_p$, with saturation of x_{Cr} in the matrix, indicates the onset of the coarsening stage, at which larger precipitates grow at the cost of the dissolution of smaller ones.

It was found that N_p^{max} increases linearly with x_{Cr} and decreases with temperature, and that the corresponding $\bar{d}_p$ stays constant at 1.4 ± 0.1 nm, for all x_{Cr} and T here studied. This means that at 'peak time' (the moment corresponding to the highest precipitate density in the system) only the density of the precipitates varies with x_{Cr} and T and not $\bar{d}_p$. To simulate precipitate-dislocation interaction at the onset of the coarsening stage, 2 nm Cr-rich precipitates were used. The densities corresponding to this size can be determined from the above presented figures.

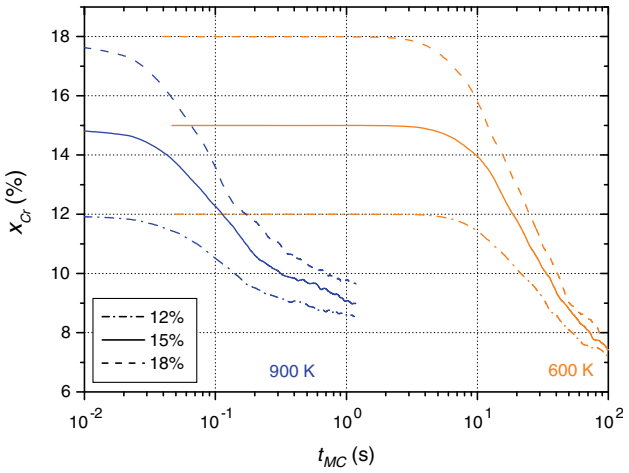

Fig. 3. The Cr-concentration in the matrix as a function of Monte Carlo simulation time.

3.2. Precipitate-dislocation interaction

The critical stress vs. precipitate size estimated from MD simulations performed at 300 K in two crystals (with $L_D = 28.9$ nm and $L_D = 41.5$ nm) for a regular square array of precipitates is shown in Fig. 4a. The critical stress, τ_C, (expressed in reduced units, $\mu b/L'$) increases linearly with d_p, consistently with results of static [15] and low temperature MD simulations [34], for this range of precipitate size and density. For larger precipitates (keeping L_D constant), when the Orowan condition is fulfilled, τ_C vs. size saturates, as proposed by Scattergood and Bacon for edge dislocations reacting with impenetrable obstacles [38], due to the self-interaction of the dislocation arms.

In Fig. 4b τ_C is plotted as a function of temperature. Clearly, τ_C scales exponentially with T in the range 300–900K. By increasing T from 300 to 900 K, the stress drops almost by a factor two for 1 nm precipitates and by about 25% for 3 nm precipitates. However, the absolute amount of stress decrease is higher for larger precipitates.

The friction flow stress for the edge dislocation moving in random Fe–Cr alloys estimated using Eq. (2) at different temperatures is shown in Fig. 5a. The estimation of the flow stress by simple averaging resulted in approximately the same value, meaning that the variation of the effective stress around its average is small. The flow stress was found to decrease from 70 to 110 MPa at room temperature down to 40–60 MPa at 900 K. These stresses are used as reference data to estimate the increase in the flow stress for an edge dislocation due to the presence of precipitates. This increase in the flow stress, $\Delta\tau$, at N_p^{max} and at the onset of the coarsening stage, was estimated using the corresponding strength coefficients for precipitate size-density distributions as obtained from AKMC simulations (see Section 3.1). The flow stress increase estimated at 600 and 900 K (temperatures considered in this study) vs. x_{Cr} is shown in Fig. 5b. In general, $\Delta\tau$ increases with x_{Cr}, and decreases with T. Indeed, the higher x_{Cr}, the higher N_p (especially at N_p^{max}), and the higher T, the lower the precipitate strength (and N_p).

The obtained results suggest that, at N_p^{max}, $\Delta\tau$ increases by about 250–300 MPa and by 180–230 MPa at 600 and 900 K, respectively. At the onset of the coarsening stage (2 nm precipitates, with density about half of N_p^{max}) a further increase of $\Delta\tau$ by about 100 Mpa

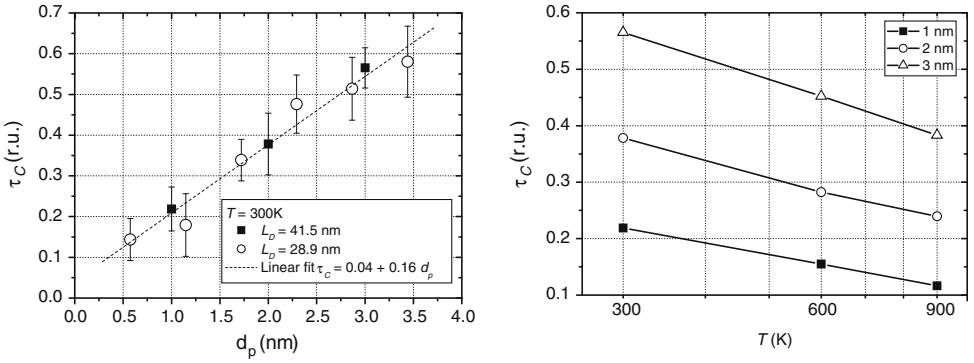

Fig. 4. The critical flow stress for the edge dislocation as a function of precipitate diameter simulated at 300 K (left) and as a function of temperature for different precipitate sizes (right).

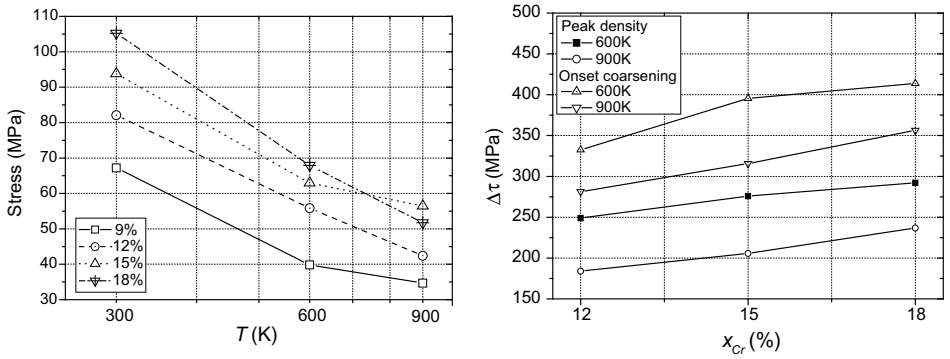

Fig. 5. The friction flow stress as a function of temperature for the edge dislocation in random alloys (left) and the flow stress increase in presence of precipitates as a function of Cr content, at different precipitation stages and at different temperatures (right).

is found, showing that the maximum hardness does not coincide with N_p^{max}.

4. Discussion

The AKMC model here-applied to trace the stages of α–α' separation is, from many points of view, an oversimplification. Some terms contributing to define the free energy of the system, notably those related to relaxation effects, are missing, as a rigid lattice energy evaluation is used. This means that contributions of vibrational entropy are neglected, which change the Cr solubility significantly at high temperature [19]. In addition, the use of the approximate formula of [28,29], with LAE-independent excess migration energy, to estimate the LAE-dependent migration barriers, is known to be an oversimplification, as shown by Djurabekova et al. [39]. The use of the real migration barriers may result in different kinetics of precipitation, thereby altering the densities and sizes of precipitates here reported. Moreover, a direct comparison of AKMC simulations with thermal ageing experiments is hindered by the lack of a safe criterion to establish the correspondence between real time and Monte Carlo time, as discussed e.g. in [32]. The solution proposed in that work is that experimental data should be used to establish the synchronisation. However, in the present case the difficulty stems from the lack of adequate experimental data. The closest experimental case to our simulations concerns relatively pure Fe–20 Cr alloys thermally aged at 793 K, reported in [6,8], where SANS was used to trace the precipitation evolution. The shortest ageing time studied was 10 h [6] and from then on only the coarsening stage was observed, thereby suggesting that our AKMC simulations correspond to an ageing time, at the corresponding temperature, on the order of a few hours. The reported density of precipitates in the experiment after 10 h is about 2×10^{25} m^{-3}, which agrees with the order of magnitude of the peak densities reported here; the experimental size is less than 2 nm in diameter, again in agreement with the present work. Thus, it may be concluded that even an oversimplified model such as the one used here, provided that the thermodynamics of the system is properly described by the applied cohesive model, is sufficient to give a reasonable description of the process of α–α' separation, not only qualitatively (the three phases of the precipitation are clearly distinguishable), but also quantitatively (the size and density are in reasonable agreement with experiments, if comparing with the proper stage of the process). Nonetheless, it appears that the calculation time required to reach the level of coarsening observed in experiments after hundreds or thousands of hours is prohibitive. In addition, the minimum density and maximum size are limited by the size of the crystal used in the simulation.

Concerning our estimates of the hardening due to α' precipitates, again it is important to be cautious with the approximations used. It is well known, for example, that Eq. (3) is valid only in the case of relatively large break-away angles (in constant line-tension approximation), when the contribution from the self-interaction of the dislocation arms is negligible. When the edge-to-edge spacing between obstacles decreases, the self-interaction becomes important and the critical stress to unpin the dislocation from an impenetrable obstacle reads [38]:

$$\tau = \frac{\mu b}{2\pi L'}(\ln(1/d_p + 1/L')^{-1} + 0.7) \tag{6}$$

From previous static (i.e. 0 K) simulations of an edge dislocation interacting with Cr-precipitates, it has been found that Eq. (3) should indeed be replaced by Eq. (6) if $L_D/d_p \leqslant 8$ for precipitates with $d_p > 3$ nm [15] and the L_D used here; otherwise Eq. (4) provides acceptable agreement. However, even though the formed precipitates were very small in size, their density was extremely high, so the condition $L_D/d_p \leqslant 8$ was not always obeyed. In addition, the effect of temperature on the self-interaction and consequently on the reduction of the stress according to Eq. (6) is so far unknown and limits its application.

Another problem is related to the actual precipitate size distribution, since at the coarsening stage the spread around the mean size increases significantly. Given that the strength of precipitates depends significantly on size (and the temperature dependence of the strength slightly varies with the size, too), the estimation of $\Delta\tau$ based on the mean size/density data is not fully rigorous. The broad size distribution means that the dislocation would move in a field of obstacles with significantly different strengths. A conventional solution to this problem is to estimate the flow stress as (for the case of two types of obstacles):

$$\tau_{1,2}^X = \tau_1^X + \tau_2^X \tag{7}$$

Here τ_1 and τ_2 are the corresponding flow stresses for the random distribution of two types of obstacles with given densities and with X varying from 1 to 2, depending on the relative obstacle strengths [40]. Taking the extreme case (upper bound) of $X = 2$, representing obstacles of comparable strengths, the flow stress estimated, for instance, in Fe–15 Cr aged at 900 K increases by ~100 MPa, as compared to mean size/density estimations, if the actual size/density distribution is used.

Clearly, both of these limitations of our estimates require, to be removed, the use of a combination of MD with larger scale, advanced approaches, such as dislocation dynamics, capable of properly allowing simultaneously for all effects of obstacle randomness, dislocation finite size and temperature. However, such a combination is not yet in place. Nevertheless, despite all the aforementioned limitations, it was found here, within the studied range of x_{Cr} and T, an increase of the flow stress (for the edge dislocation) of 170–270 MPa at the peak density and 270–420 MPa at the onset of coarsening stage. These values are not incompatible with the values of yield stress increase reported in [4] for Fe–14 Cr and Fe–18 Cr alloys, thermally aged for 4800 h at 700 K and for 1488 h at 811 K, which amount to about 170 MPa (811 K) and 270 MPa (700 K) for the former alloy and to about 200 MPa (811 K) and 490 MPa (700 K) for the latter. No microstructural information is provided in the cited work, but it can reasonably be estimated, by comparison with other available experiments [6,8–10], that after such long annealing the precipitates will be significantly larger and with densities about two orders of magnitude lower. Therefore this comparison should only provide an estimate for the order of magnitude of the yield stress increase.

5. Conclusions

A multi-scale modelling approach was followed to investigate effects on mechanical properties from α–α' phase separation in Fe–Cr alloys relevant for structural nuclear applications. To do so, a DFT-based interatomic potential was used in AKMC and MD studies to simulate thermal ageing and the effect of phase separation on the dislocation motion, respectively.

In the AKMC studies the peak density was found to vary with T and x_{Cr} in the range 10^{24}–10^{25} m^{-3} but the average precipitate size (at the moment when the maximum N_p is reached) remains the same ($\bar{d}_p = 1.4$ nm) within the error bar. The obtained size and density distributions are in the range of experimental observations.

Within the x_{Cr} and T range of this study, the increase of the flow stress for the edge dislocation is found to vary in the range of 170–270 MPa for the peak density and 270–420 MPa at the onset of coarsening stage, depending on x_{Cr} and T. In general, the higher x_{Cr}, the higher the increase in flow stress and vice versa for T. It was found that the peak hardening does not correspond with the

peak density and further phase separation results in a further increase of the flow stress. The flow stress increase obtained from our simulations is found to be within the range of experimental observations. The main limitation of our combination of models consists in the prohibitive CPU time and box size required to simulate coarsening up to the level experimentally observed after thousands of hours. This coarsening level is reached much faster under irradiation and is therefore of relevance for nuclear applications. The open challenge is thus to develop similar models capable of tracing the evolution of phase separation under irradiation conditions.

Acknowledgements

This work was performed in the framework of the 7th Framework Programme project GETMAT, partially supported by the European Commission. It also contributes to the European Fusion Technology programme (EFDA).

References

[1] R.M. Fisher, E.J. Dulis, K.G. Carroll, Trans. AIME 197 (1953) 690.
[2] R.O. Williams, H.W. Paxton, J. Iron Steel I. 185 (1957) 358.
[3] R. Lagneborg, Trans. ASM 60 (1967) 67.
[4] P.J. Grobner, Metall. Trans. 4 (1973) 251.
[5] P. Jacobsson, Y. Bergström, B. Aronsson, Metall. Trans. 6A (1977) 1577.
[6] F. Bley, Acta Metall. Mater. 40 (1992) 1505.
[7] P. Dubuisson, D. Gilbon, J.L. Séran, J. Nucl. Mater. 205 (1993) 178.
[8] V. Jaquet, PhD. thesis, Ecole Polytechnique, Palaiseau, France (6 March 2000).
[9] M.H. Mathon, Y. De Carlan, G. Geoffroy, X. Averty, C.H. de Novion, A. Alamo, in: S.T. Rosinski, M.L. Grossbeck, T.R. Allen, A.S. Kumar (Eds.), Effects of Radiation on Materials: 20th International Symposium, ASTM STP 1405, American Society for Testing and Materials, West Conshohocken, PA, 2001, p. 674.
[10] M.H. Mathon, Y. de Carlan, G. Geoffroy, X. Averty, A. Alamo, C.H. de Novion, J. Nucl. Mater. 312 (2003) 236.
[11] E.A. Little, D.A. Stow, J. Nucl. Mater. 87 (1979) 25.
[12] E. Wakai, A. Hishinuma, Y. Kato, H. Yano, S. Takaki, K. Abiko, J. Physique IV 05 C7 (1995) 277.
[13] E. Wakai, A. Hishinuma, K. Usami, Y. Kato, S. Takaki, K. Abiko, Mater. Trans. Japan Inst. Met. 41 (2000) 1180.
[14] F. Danoix, P. Auger, Mater. Charact. 44 (2000) 177.
[15] D.A. Terentyev, G. Bonny, L. Malerba, Acta Mater. 56 (2008) 3229.
[16] T.P.C. Klaver, R. Drautz, M.W. Finnis, Phys. Rev. B 74 (2006) 094435.
[17] P. Olsson, I.A. Abrikosov, J. Wallenius, J. Nucl. Mater. 321 (2003) 84.
[18] P. Olsson, I.A. Abrikosov, J. Wallenius, Phys. Rev. B 73 (2006) 104416.
[19] G. Bonny, R.C. Pasianot, L. Malerba, A. Caro, P. Olsson, M. Lavrentiev, J. Nucl. Mater. 385 (2009) 268.
[20] A. Caro, D.A. Crowson, M. Caro, Phys. Rev. Lett. 95 (2005) 75702.
[21] [a] P. Olsson, J. Wallenius, C. Domain, K. Nordlund, L. Malerba, Phys. Rev. B 72 (2005) 214119;
[b] P. Olsson, J. Wallenius, C. Domain, K. Nordlund, L. Malerba, Phys. Rev. B 74 (2006) 1(E).
[22] M.Y. Lavrentiev, R. Drautz, D. Nguyen-Manh, T.P.C. Klaver, S.L. Dudarev, Phys. Rev. B 75 (2007) 14208.
[23] M.S. Daw, M.I. Baskes, Phys. Rev. B 29 (1984) 6443.
[24] G. Bonny, D. Terentyev, L. Malerba, Comput. Mater. Sci. 42 (2008) 107.
[25] S.S. Brenner, M.K. Miller, W.A. Soffa, Scr. Metall. 16 (1982) 831.
[26] H. Kuwano, Trans. Japan Inst. Met. 26 (1985) 473.
[27] S.M. Dubiel, G. Inden, Z. Metallkde. 78 (1987) 544.
[28] C. Domain, C.S. Becquart, J.C. Van Duysen, Mater. Res. Soc. Symp. Proc. 650 (2001) R3.25.1.
[29] H.C. Kang, W.H. Weinberg, J. Chem. Phys. 90 (1989) 2824.
[30] P. Olsson, C. Domain, J. Wallenius, Phys. Rev. B 75 (2007) 014110.
[31] W.M. Young, E.W. Elcock, Proc. Phys. Soc. 89 (1966) 735.
[32] E. Vincent, C.S. Becquart, C. Pareige, P. Pareige, C. Domain, J. Nucl. Mater. 373 (2008) 387.
[33] Yu.N. Osetsky, D.J. Bacon, V. Mohles, Philos. Mag. 1 (2003) 3623.
[34] D. Terentyev, G. Bonny, L. Malerba, Mobility of dislocations in thermal aged and irradiated Fe–Cr alloys, Proc. ICFRM-13, J. Nucl. Mater. accepted for publication.
[35] C. Domain, G. Monnet, Phys. Rev. Lett. 95 (2005) 215506.
[36] J. Friedel, Dislocations, Pergamon, Oxford, 1964.
[37] D. Terentyev, G. Bonny, L. Malerba, Characterization of voids and precipitates as competing sources of hardening in irradiated Fe–9Cr alloys, J. Nucl. Mater. submitted for publication.
[38] R.O. Scattergood, D.J. Bacon, Acta Metall. 30 (1982) 1665.
[39] F.G. Djurabekova, R. Domingos, G. Cerchiara, N. Castin, E. Vincent, L. Malerba, Nucl. Instr. Meth. Phys. Res. B 255 (2007) 8.
[40] F.J. Humphreys, Dislocation–particle interaction, in: Dislocations and properties of real materials, Institute of Metals, London, 1985.